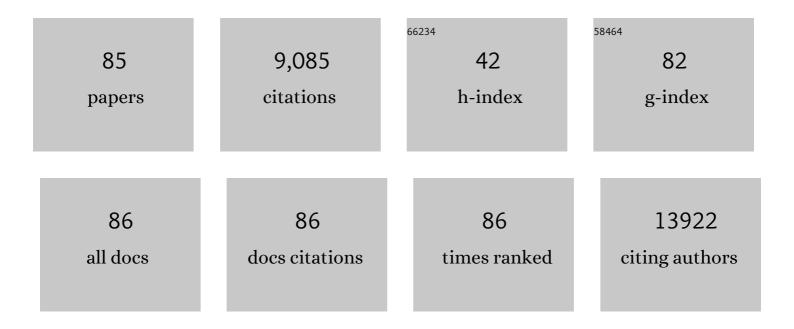
List of Publications by Year in descending order

Source: https://exaly.com/author-pdf/4295934/publications.pdf Version: 2024-02-01



YUNG-CHANGLIN

#	Article	IF	CITATIONS
1	Composition and phase engineering of metal chalcogenides and phosphorous chalcogenides. Nature Materials, 2023, 22, 450-458.	13.3	62
2	Imaging of isotope diffusion using atomic-scale vibrational spectroscopy. Nature, 2022, 603, 68-72.	13.7	14
3	Formation of Highly Doped Nanostripes in 2D Transition Metal Dichalcogenides via a Dislocation Climb Mechanism. Advanced Materials, 2021, 33, e2007819.	11.1	13
4	Two-dimensional iodine-monofluoride epitaxy on WSe2. Npj 2D Materials and Applications, 2021, 5, .	3.9	5
5	Embedment of Multiple Transition Metal Impurities into WS ₂ Monolayer for Bandstructure Modulation. Small, 2021, 17, e2007171.	5.2	6
6	Tunable Doping of Rhenium and Vanadium into Transition Metal Dichalcogenides for Twoâ€Dimensional Electronics. Advanced Science, 2021, 8, e2004438.	5.6	66
7	Mixed-Salt Enhanced Chemical Vapor Deposition of Two-Dimensional Transition Metal Dichalcogenides. Chemistry of Materials, 2021, 33, 7301-7308.	3.2	22
8	One-step synthesis of BaTiO ₃ /CaTiO ₃ core-shell nanocubes by hydrothermal reaction. Journal of Asian Ceramic Societies, 2021, 9, 359-365.	1.0	5
9	Polymorphic Phases of Metal Chlorides in the Confined 2D Space of Bilayer Graphene. Advanced Materials, 2021, 33, e2105898.	11.1	12
10	Optoelectronic Properties of Atomically Thin MoxW(1â^'x)S2 Nanoflakes Probed by Spatially-Resolved Monochromated EELS. Nanomaterials, 2021, 11, 3218.	1.9	6
11	Coupling and Decoupling of Bilayer Graphene Monitored by Electron Energy Loss Spectroscopy. Nano Letters, 2021, 21, 10386-10391.	4.5	10
12	Polymorphic Phases of Metal Chlorides in the Confined 2D Space of Bilayer Graphene (Adv. Mater.) Tj ETQq0 0 C	rgBT /Ove	erlock 10 Tf 5
13	Graphene–Transition Metal Dichalcogenide Heterojunctions for Scalable and Low-Power Complementary Integrated Circuits. ACS Nano, 2020, 14, 985-992.	7.3	46
14	Templateâ€Assisted Synthesis of Metallic 1T′â€&n _{0.3} W _{0.7} S ₂ Nanosheets for Hydrogen Evolution Reaction. Advanced Functional Materials, 2020, 30, 1906069.	7.8	47
15	Dualâ€Metal Interbonding as the Chemical Facilitator for Singleâ€Atom Dispersions. Advanced Materials, 2020, 32, e2003484.	11.1	90
16	Twist Angle-Dependent Optical Responses in Controllably Grown WS ₂ Vertical Homojunctions. Chemistry of Materials, 2020, 32, 9721-9729.	3.2	25
17	Seamlessly Splicing Metallic Sn <i>_x</i> Mo _{1â~} <i>_x</i> S ₂ at MoS ₂ Edge for Enhanced Photoelectrocatalytic Performance in Microreactor. Advanced Science, 2020, 7, 2002172.	5.6	30

Blue emission at atomically sharp 1D heterojunctions between graphene and h-BN. Nature Communications, 2020, 11, 5359.

#	Article	IF	CITATIONS
19	Scalable T-Gate Aligned Gr–WS ₂ –Gr Radio-Frequency Field-Effect Transistors. ACS Applied Electronic Materials, 2020, 2, 3898-3905.	2.0	11
20	Isothermal Growth and Stacking Evolution in Highly Uniform Bernal-Stacked Bilayer Graphene. ACS Nano, 2020, 14, 6834-6844.	7.3	28
21	Direct observation and catalytic role of mediator atom in 2D materials. Science Advances, 2020, 6, eaba4942.	4.7	7
22	Direct Growth of Wafer-Scale, Transparent, p-Type Reduced-Graphene-Oxide-like Thin Films by Pulsed Laser Deposition. ACS Nano, 2020, 14, 3290-3298.	7.3	20
23	Photogating WS ₂ Photodetectors Using Embedded WSe ₂ Charge Puddles. ACS Nano, 2020, 14, 4559-4566.	7.3	87
24	Scanning Moiré Fringe Method: A Superior Approach to Perceive Defects, Interfaces, and Distortion in 2D Materials. ACS Nano, 2020, 14, 6034-6042.	7.3	13
25	Wafer-scale and deterministic patterned growth of monolayer MoS ₂ <i>via</i> viavapor–liquid–solid method. Nanoscale, 2019, 11, 16122-16129.	2.8	76
26	Synthesis of sub-millimeter single-crystal grains of aligned hexagonal boron nitride on an epitaxial Ni film. Nanoscale, 2019, 11, 14668-14675.	2.8	16
27	Layer Rotation-Angle-Dependent Excitonic Absorption in van der Waals Heterostructures Revealed by Electron Energy Loss Spectroscopy. ACS Nano, 2019, 13, 9541-9550.	7.3	25
28	Vapor Phase Selective Growth of Two-Dimensional Perovskite/WS ₂ Heterostructures for Optoelectronic Applications. ACS Applied Materials & amp; Interfaces, 2019, 11, 40503-40511.	4.0	39
29	Synthesis and Transport Properties of Degenerate P-Type Nb-Doped WS ₂ Monolayers. Chemistry of Materials, 2019, 31, 3534-3541.	3.2	71
30	Ultrafast Monolayer In/Gr-WS ₂ -Gr Hybrid Photodetectors with High Gain. ACS Nano, 2019, 13, 3269-3279.	7.3	44
31	Isolation of Single-Wired Transition-Metal Monochalcogenides by Carbon Nanotubes. Nano Letters, 2019, 19, 4845-4851.	4.5	61
32	Vapour–liquid–solid growth of monolayer MoS2 nanoribbons. Nature Materials, 2018, 17, 535-542.	13.3	286
33	Hydrogen-Assisted Epitaxial Growth of Monolayer Tungsten Disulfide and Seamless Grain Stitching. Chemistry of Materials, 2018, 30, 403-411.	3.2	60
34	Revealing the Atomic Defects of WS ₂ Governing Its Distinct Optical Emissions. Advanced Functional Materials, 2018, 28, 1704210.	7.8	69
35	Stable 1T Tungsten Disulfide Monolayer and Its Junctions: Growth and Atomic Structures. ACS Nano, 2018, 12, 12080-12088.	7.3	74
36	Surface-Mediated Aligned Growth of Monolayer MoS ₂ and In-Plane Heterostructures with Graphene on Sapphire. ACS Nano, 2018, 12, 10032-10044.	7.3	64

#	Article	IF	CITATIONS
37	Selective Growth of Two-Dimensional Heterostructures of Gallium Selenide on Monolayer Graphene and the Thickness Dependent <i>p-</i> and <i>n-</i> Type Nature. ACS Applied Nano Materials, 2018, 1, 3293-3302.	2.4	9
38	MoS2 monolayer catalyst doped with isolated Co atoms for the hydrodeoxygenation reaction. Nature Chemistry, 2017, 9, 810-816.	6.6	683
39	Unexpected Huge Dimerization Ratio in One-Dimensional Carbon Atomic Chains. Nano Letters, 2017, 17, 494-500.	4.5	35
40	Scalable van der Waals Heterojunctions for High-Performance Photodetectors. ACS Applied Materials & Interfaces, 2017, 9, 36181-36188.	4.0	29
41	Optical Spectroscopy at High Spatial Resolution with Fast Electrons. Microscopy and Microanalysis, 2017, 23, 1528-1529.	0.2	Ο
42	Towards atomically precise manipulation of 2D nanostructures in the electron microscope. 2D Materials, 2017, 4, 042004.	2.0	73
43	Single Atomically Sharp Lateral Monolayer pâ€n Heterojunction Solar Cells with Extraordinarily High Power Conversion Efficiency. Advanced Materials, 2017, 29, 1701168.	11.1	111
44	Monochromated EELS to Probe the Local Optical Properties of Low-Dimensional Materials. Microscopy and Microanalysis, 2016, 22, 950-951.	0.2	0
45	Gentle transfer method for water- and acid/alkali-sensitive 2D materials for (S)TEM study. APL Materials, 2016, 4, .	2.2	12
46	Electron energy loss spectroscopy of excitons in two-dimensional-semiconductors as a function of temperature. Applied Physics Letters, 2016, 108, .	1.5	14
47	Postsynthesis of hâ€BN/Graphene Heterostructures Inside a STEM. Small, 2016, 12, 252-259.	5.2	23
48	Atomic Structure and Spectroscopy of Single Metal (Cr, V) Substitutional Dopants in Monolayer MoS ₂ . ACS Nano, 2016, 10, 10227-10236.	7.3	96
49	Dynamic Structural Evolution of Metal–Metal Bonding Network in Monolayer WS ₂ . Chemistry of Materials, 2016, 28, 2308-2314.	3.2	37
50	Photoluminescence Enhancement and Structure Repairing of Monolayer MoSe ₂ by Hydrohalic Acid Treatment. ACS Nano, 2016, 10, 1454-1461.	7.3	179
51	Secondary electron imaging of monolayer materials inside a transmission electron microscope. Applied Physics Letters, 2015, 107, 063105.	1.5	3
52	Exciton Mapping at Subwavelength Scales in Two-Dimensional Materials. Physical Review Letters, 2015, 114, 107601.	2.9	79
53	Structure and Local Chemical Properties of Boron-Terminated Tetravacancies in Hexagonal Boron Nitride. Physical Review Letters, 2015, 114, 075502.	2.9	33
54	Inelastic electron irradiation damage in hexagonal boron nitride. Micron, 2015, 72, 21-27.	1.1	28

YUNG-CHANG LIN

#	Article	IF	CITATIONS
55	Epitaxial growth of a monolayer WSe ₂ -MoS ₂ lateral p-n junction with an atomically sharp interface. Science, 2015, 349, 524-528.	6.0	1,009
56	Influence of rhenium on the structural and optical properties of molybdenum disulfide. Japanese Journal of Applied Physics, 2015, 54, 04DH05.	0.8	21
57	Temperature Dependence of the Reconstruction of Zigzag Edges in Graphene. ACS Nano, 2015, 9, 4786-4795.	7.3	68
58	Three-fold rotational defects in two-dimensional transition metal dichalcogenides. Nature Communications, 2015, 6, 6736.	5.8	179
59	Single-Layer ReS ₂ : Two-Dimensional Semiconductor with Tunable In-Plane Anisotropy. ACS Nano, 2015, 9, 11249-11257.	7.3	353
60	Characterization of Graphene and Transition Metal Dichalcogenide at the Atomic Scale. Journal of the Physical Society of Japan, 2015, 84, 121005.	0.7	6
61	Structural and Chemical Dynamics of Pyridinic-Nitrogen Defects in Graphene. Nano Letters, 2015, 15, 7408-7413.	4.5	204
62	Exploring the Single Atom Spin State by Electron Spectroscopy. Physical Review Letters, 2015, 115, 206803.	2.9	80
63	In situ observation of step-edge in-plane growth of graphene in a STEM. Nature Communications, 2014, 5, 4055.	5.8	55
64	Composition dependent lattice dynamics in MoS <i>x</i> Se(2– <i>x</i>) alloys. Journal of Applied Physics, 2014, 116, .	1.1	35
65	Atomic mechanism of the semiconducting-to-metallic phase transition in single-layered MoS2. Nature Nanotechnology, 2014, 9, 391-396.	15.6	1,146
66	Properties of Individual Dopant Atoms in Single‣ayer MoS ₂ : Atomic Structure, Migration, and Enhanced Reactivity. Advanced Materials, 2014, 26, 2857-2861.	11.1	258
67	Stability and Spectroscopy of Single Nitrogen Dopants in Graphene at Elevated Temperatures. ACS Nano, 2014, 8, 11806-11815.	7.3	45
68	Atomic Level Spatial Variations of Energy States along Graphene Edges. Nano Letters, 2014, 14, 6155-6159.	4.5	33
69	Gating Electron–Hole Asymmetry in Twisted Bilayer Graphene. ACS Nano, 2014, 8, 6962-6969.	7.3	22
70	Probing interlayer coupling in twisted singleâ€crystal bilayer graphene by Raman spectroscopy. Journal of Raman Spectroscopy, 2014, 45, 912-917.	1.2	12
71	Growth and Raman Spectra of Single-Crystal Trilayer Graphene with Different Stacking Orientations. ACS Nano, 2014, 8, 10766-10773.	7.3	56
72	Evidence for Active Atomic Defects in Monolayer Hexagonal Boron Nitride: A New Mechanism of Plasticity in Two-Dimensional Materials. Nano Letters, 2014, 14, 1064-1068.	4.5	90

#	Article	IF	CITATIONS
73	Controllable Synthesis of Band-Gap-Tunable and Monolayer Transition-Metal Dichalcogenide Alloys. Frontiers in Energy Research, 2014, 2, .	1.2	84
74	Low-temperature synthesis of graphene on Cu using plasma-assisted thermal chemical vapor deposition. Nanoscale Research Letters, 2013, 8, 285.	3.1	60
75	Twisting Bilayer Graphene Superlattices. ACS Nano, 2013, 7, 2587-2594.	7.3	173
76	High Mobility Flexible Graphene Field-Effect Transistors with Self-Healing Gate Dielectrics. ACS Nano, 2012, 6, 4469-4474.	7.3	169
77	Remote Catalyzation for Direct Formation of Graphene Layers on Oxides. Nano Letters, 2012, 12, 1379-1384.	4.5	146
78	Graphene Annealing: How Clean Can It Be?. Nano Letters, 2012, 12, 414-419.	4.5	801
79	Metalâ€Free Growth of Nanographene on Silicon Oxides for Transparent Conducting Applications. Advanced Functional Materials, 2012, 22, 2123-2128.	7.8	150
80	Characterization of Graphene Grown on Bulk and Thin Film Nickel. Langmuir, 2011, 27, 13748-13753.	1.6	17
81	Clean Transfer of Graphene for Isolation and Suspension. ACS Nano, 2011, 5, 2362-2368.	7.3	285
82	Tuning of Charge Densities in Graphene by Molecule Doping. Advanced Functional Materials, 2011, 21, 2687-2692.	7.8	99
83	Defect Engineering for Graphene Tunable Doping. Materials Research Society Symposia Proceedings, 2011, 1283, 1.	0.1	Ο
84	Tailoring point electron sources of individual carbon nanotubes. Applied Physics Letters, 2010, 97, 073119.	1.5	3
85	Controllable graphene N-doping with ammonia plasma. Applied Physics Letters, 2010, 96, .	1.5	446